Accepted Manuscript

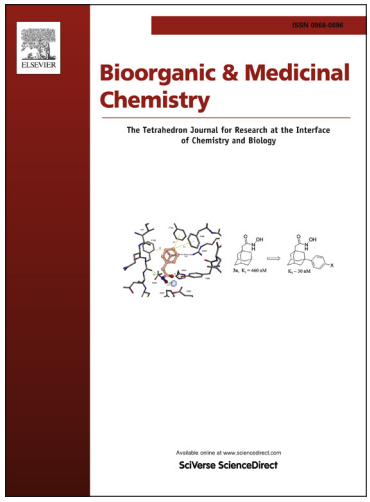

Australian marine sponge alkaloids as a new class of glycine-gated chloride channel receptor modulator

Walter Balansa, Robiul Islam, Daniel F. Gilbert, Frank Fontaine, Xue Xiao, Hua Zhang, Andrew M. Piggott, Joseph W. Lynch, Robert J. Capon

PII: S0968-0896(13)00387-8
DOI: http://dx.doi.org/10.1016/j.bmc.2013.04.061
Reference: BMC 10801

To appear in: *Bioorganic & Medicinal Chemistry*

Received Date: 25 February 2013
Revised Date: 10 April 2013
Accepted Date: 18 April 2013

Please cite this article as: Balansa, W., Islam, R., Gilbert, D.F., Fontaine, F., Xiao, X., Zhang, H., Piggott, A.M., Lynch, J.W., Capon, R.J., Australian marine sponge alkaloids as a new class of glycine-gated chloride channel receptor modulator, *Bioorganic & Medicinal Chemistry* (2013), doi: http://dx.doi.org/10.1016/j.bmc.2013.04.061

Graphical Abstract

To create your abstract, type over the instructions in the template box below.
Fonts or abstract dimensions should not be changed or altered.

Australian marine sponge alkaloids as a new class of glycine-gated chloride channel receptor modulator

Leave this area blank for abstract info.

Walter Balansa, Robiul Islam, Daniel F. Gilbert, Frank Fontaine, Xue Xiao, Hua Zhang, Andrew M. Piggott, Joseph W. Lynch* and Robert J. Capon*

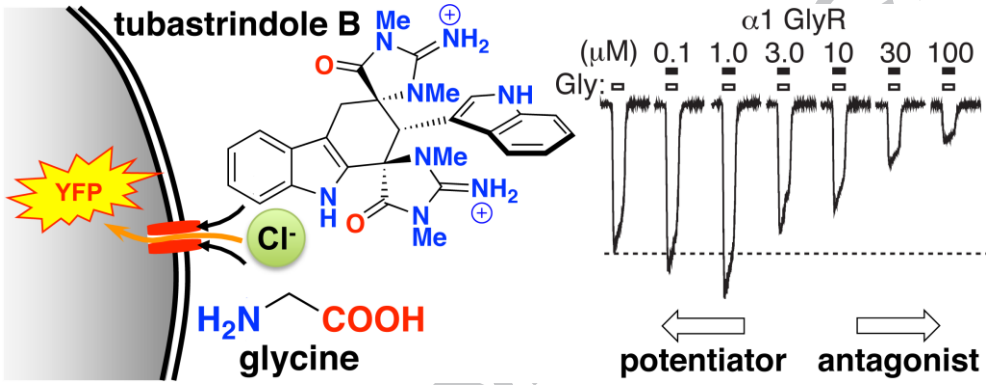

Bioorganic & Medicinal Chemistry
journal homepage: www.elsevier.com

Australian marine sponge alkaloids as a new class of glycine-gated chloride channel receptor modulator

Walter Balansa,[a§] Robiul Islam,[b§] Daniel F. Gilbert,[b] Frank Fontaine,[a] Xue Xiao,[a] Hua Zhang,[a] Andrew M. Piggott,[a] Joseph W. Lynch[b,c]* and Robert J. Capon[a]*

[a] *Institute for Molecular Bioscience, The University of Queensland, St. Lucia, QLD, 4072, Australia*
[b] *Queensland Brain Institute, The University of Queensland, St. Lucia, QLD, 4072, Australia*
[c] *School of Biomedical Sciences, The University of Queensland, St. Lucia, QLD, 4072, Australia*

ARTICLE INFO

Article history:
Received
Revised
Accepted
Available online

Keywords:
glycine-gated chloride channel receptor modulators
sesterterpene tetronic acid glycinyl lactams
Ianthella cf. flabelliformis
marine natural products chemistry

ABSTRACT

Chemical analysis of a specimen of the sponge *Ianthella* cf. *flabelliformis* returned two new sesquiterpene glycinyl lactams, ianthellalactams A (**1**) and B (**2**), the known sponge sesquiterpene dictyodendrillin (**3**) and its ethanolysis artifact ethyl dictyodendrillin (**4**), and five known sponge indole alkaloids, aplysinopsin (**5**), 8*E*-3′-deimino-3′-oxoaplysinopsin (**6**), 8*Z*-3′-deimino-3′-oxoaplysinopsin (**7**), dihydroaplysinopsin (**8**) and tubastrindole B (**9**). The equilibrated mixture **6**/**7** exhibited glycine-gated chloride channel receptor (GlyR) antagonist activity with a bias towards α3 over α1 GlyR, while tubastrindole B (**9**) exhibited a bias towards α1 over α3 GlyR. At low- to sub-micromolar concentrations, **9** was also a selective potentiator of α1 GlyR, with no effect on α3 GlyR – a pharmacology that could prove useful in the treatment of movement disorders such as spasticity and hyperekplexia (pronounced startle response). Our investigations into the GlyR modulatory properties of **1**–**9** were further supported by the synthesis of a number of structurally related indole alkaloids.

1. Introduction

Glycine-gated chloride channel receptors (GlyRs) are members of the Cys-loop ion channel receptor family comprising subunits α1–α4 and β. They play a pivotal role in orchestrating inhibitory neurotransmission in the spinal cord, brainstem and retina,[1] with functional GlyRs being formed either as pentameric homomers or as αβ heteromers. GlyR subunits exhibit differential central nervous system distributions that are particularly evident in the superficial dorsal horn of the spinal cord[2] and the retina.[3-6] The physiological consequences of differential distribution patterns are difficult to establish as there are currently few pharmacological probes that can selectively inhibit different GlyR isoforms,[7] and therefore small molecule isoform-selective GlyRs modulators (agonists, antagonists, potentiators) would have significant value as both pharmacological tools and as lead compounds for inflammatory pain,[2,8] opioid-induced breathing disorders,[9] epilepsy[10] and movement disorders.[11] In an attempt to address this need, we recently screened a library of >2,500 southern Australian and Antarctic marine invertebrates and algae for metabolites displaying GlyR-modulating properties. This approach successfully identified a number of promising extracts, and in a preliminary report[12] we described sesterterpene tetronic acid glycinyl-lactams from several *Ircinia* spp., as a new class of isoform selective GlyR modulators. This report extends on our earlier findings and details the chemical analysis of a specimen of the GlyR-active sponge *Ianthella* cf. *flabelliformis*.

2. Results and Discussion

A portion of the EtOH extract of *Ianthella* cf. *flabelliformis* was decanted, dried *in vacuo* and subjected to solvent partitioning and trituration. The GlyR-modulatory CH_2Cl_2- and MeOH-soluble materials were further fractionated by reversed phase HPLC to yield two new sesquiterpene lactams ianthellalactams A (**1**) and B (**2**), the known sponge sesquiterpene dictyodendrillin[13] (**3**), its ethanolysis artifact ethyl dictyodendrillin (**4**), and five known sponge indole alkaloids, aplysinopsin[14] (**5**), 8*E*-3′-deimino-3′-oxoaplysinopsin[15] (**6**), 8*Z*-3′-deimino-3′-oxoaplysinopsin[15] (**7**), dihydroaplysinopsin[16] (**8**) and tubastrindole B[17] (**9**) (Figure 1). The compounds **3**–**9** were characterized by detailed spectroscopic analysis and comparison with literature data (see Supporting Information).

High resolution ESI(+)MS analysis of **1** and **2** revealed quasi-molecular ions $[M+H]^+$ consistent with isomeric molecular formulae ($C_{17}H_{25}NO_3$) incorporating six double bond equivalents (DBE). Analysis of the 1D and 2D NMR (methanol-d_4) data for **1** and **2** (Table 1 and Figure 2) revealed resonances and correlations consistent with common geranyl and glycinyl residues, and differing trisubstituted α,β-unsaturated esters/lactones. These observations account for five DBE and require that both **1** and **2** be monocyclic. Diagnostic deshielded C-19 resonances supported assignment of *E* $\Delta^{7,8}$ configurations for **1** (δ_C 16.3) and **2** (δ_C 16.3), further confirmed by comparison to authentic samples of the closely related dictyodendrillin (**3**) and

* Corresponding authors. JWL: Tel: +61-7-3346-6375; fax: +61-7-3346-6301; e-mail: j.lynch@uq.edu.au; RJC: Tel.: +61-7-3346-2979; fax: +61-7-3346-2090; e-mail: r.capon@uq.edu.au; § These authors contributed equally to this work

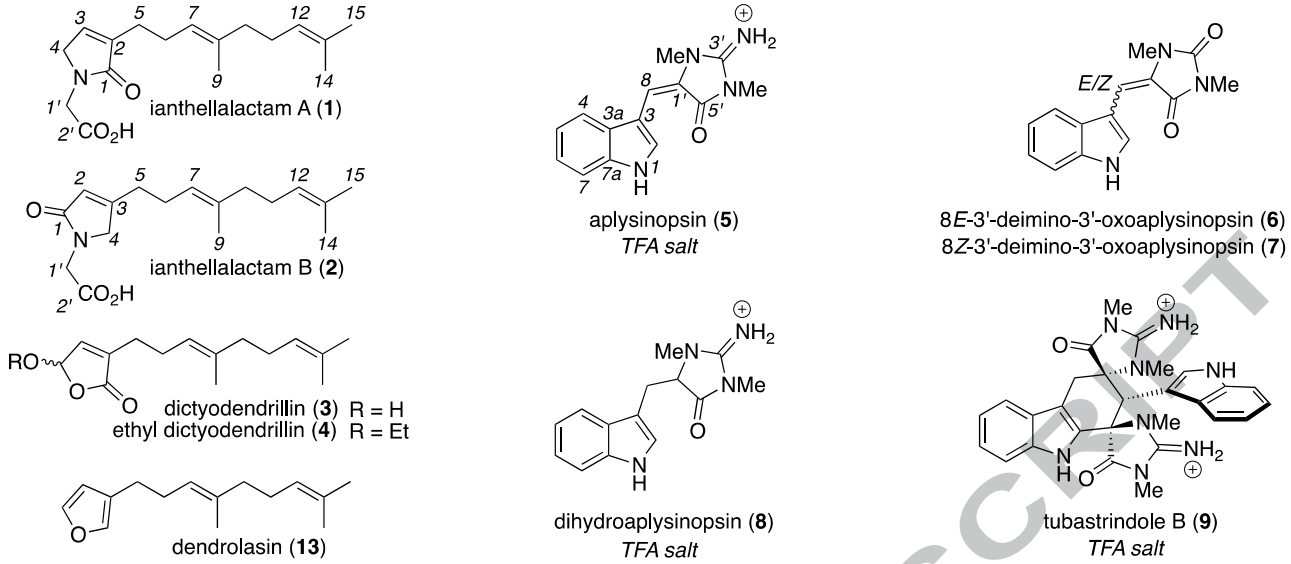

Figure 1. *Ianthella* cf. *flabelliformis* metabolites **1**–**9**, and dendrolasin (**13**)

dendrolasin (**13**). HMBC correlations and significant deshielding of H-3 in **1** (δ_H 6.88) compared to H-2 in **2** (δ_H 5.85) confirmed the presence of regioisomeric glycinyl lactam moieties. Thus the complete structures for ianthellalactams A (**1**) and B (**2**) were assigned as shown.

Although **1** and **2** possess a rare glycinyl lactam moiety in common with the ircinialactams[12] (marine sponge metabolites previously reported by us as potent GlyR modulators), neither **1** nor **2** exhibited any effect against either α1 or α3 GlyRs. Indeed, following a comprehensive testing of all metabolites the GlyR modulatory activity detected in the crude *Ianthella* cf. *flabelliformis* extract was attributed solely to **6**/**7**, and **9** (Figure 3 and Table 2). Whereas the (photo-activated) equilibrating mixture of geometric isomers **6**/**7** exhibited weak GlyR antagonist activity with a modest bias towards α3 over α1, the dimeric analog tubastrindole B (**9**) proved to be a more potent GlyR antagonist with a bias towards α1 over α3. Of interest, **9** was found to be a selective potentiator of α1 GlyR at low- to sub-μM concentrations (126 ± 5% at 1 μM), while exhibiting no such effect on α3 GlyR – a pharmacology that could prove useful as a treatment for movement disorders such as spasticity and hyperekplexia (pronounced startle response). This unusual difference in activity at lower and high concentrations suggests **9** may have two distinct α1 GlyR binding sites.

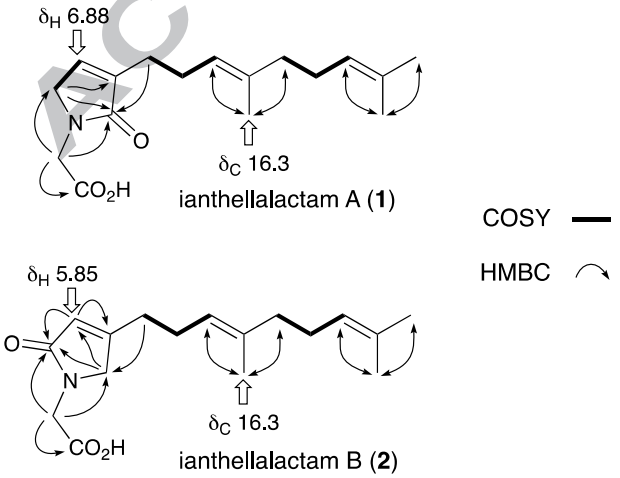

Figure 2. Diagnostic NMR (methanol-d_4) resonances and correlations for **1** and **2**

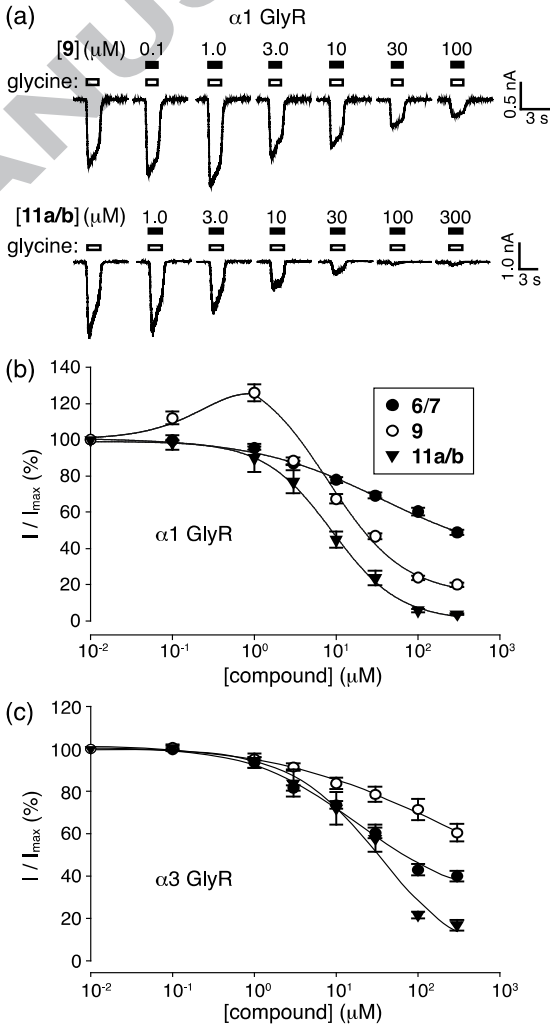

Figure 3. Electrophysiological analysis of **6**/**7**, **9** and **11a**/**b** on α1 and α3 GlyRs. (a) Sample dose-responses of **9** and **11a/b** on currents activated by EC_{50} glycine at α1 GlyR. (b) Averaged dose-responses of the 3 compounds at α1 GlyR and (c) α3 GlyR. Mean parameters of best fit to individual inhibitory dose-response relationships are presented in Table 1. Curve fits represent Hill equation fits to averaged data only and these parameters were not used for analysis. An exception is the biphasic curve fit to the **11a/b** data at the α1 GlyR, which was fit by the sum of two Hill equations.

Table 1. ^{1}H (600 MHz) and ^{13}C (150 MHz) NMR data for ianthellalactams A (**1**) and B (**2**) in methanol-d_4

Position	ianthellalactam A (**1**)		ianthellalactam B (**2**)	
	δ_H, mult. (*J* in Hz)	δ_C[a]	δ_H, mult. (*J* in Hz)	δ_C[a]
1		174.4		175.0
2		139.7	5.85, tt (1.4, 1.4)	121.5
3	6.88, tt (1.6, 1.6)	138.9		164.6
4	4.05, dt (1.6, 1.6)	53.1	4.11, d (1.4)	56.8
5	2.29[b]	27.1	2.48, td (7.4, 1.4)	30.8
6	2.27[b]	27.2	2.30, br td (7.4, 7.1)	27.4
7	5.16, tq (6.9, 1.3)	124.8	5.16, tq (7.1, 1.3)	124.3
8		137.3		137.9
9	1.60, br s	16.3	1.64, br s	16.3
10	1.99, br t (7.6)	41.0	2.00, br t (7.6)	40.9
11	2.08, br td (7.6, 7.0)	27.9	2.08, br td (7.6, 7.0)	27.8
12	5.09, tqq (7.0, 1.4, 1.4)	125.6	5.08, tqq (7.0, 1.4, 1.4)	125.4
13		132.3		132.4
14	1.60, br s	17.9	1.60, br s	17.9
15	1.67, br s	26.0	1.66, br s	26.0
1′	4.21, s	44.9	4.17, s	44.4
2′		173.0		172.9

[a] ^{13}C NMR assignments supported by HSQC data; [b] overlapping resonances.

To further probe the indole alkaloid GlyR pharmacophore exemplified by **6/7** and **9**, we employed aldol condensations to couple indole-3-carboxaldehyde with hydantoin, methyl hydantoin and creatinine, to synthesize the analogs **10**, **11a/b** and **12a/b** respectively (Figure 4). Significantly, whereas the unmethylated hydantoin derived alkaloid **10** was prepared as the stable *E* isomer, the methylated analogs **11a** and **11b** derived from methyl hydantoin, and **12a** and **12b** derived from creatinine, existed as photo-labile equilibrating mixtures of geometric isomers. These analogs were exposed to UV light for 3 h prior to bioassay to generate ~1:1 mixtures of the *E*:*Z* isomers. Of note, only the mixture **11a/b** exhibited significant GlyR modulatory activity, being a more a potent GlyR antagonist than either **6/7** or **9**, with a bias favoring α1 over α3 (Figure 3 and Table 2).

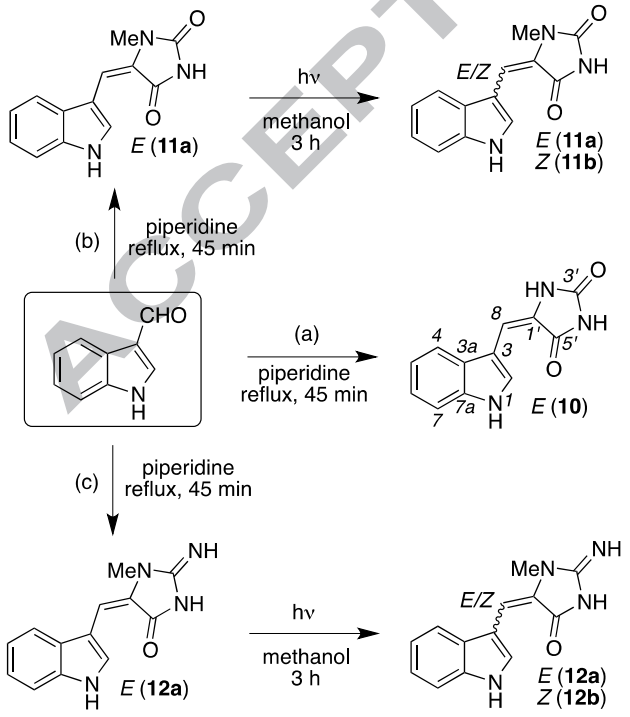

Figure 4. Synthesis of indole alkaloid analogs. (a) hydantoin; (b) methylhydantoin; (c) creatinine.

Table 2. Automated electrophysiology (concentration dependence) of **6/7**, **9** and **11a/b** on stably expressed α1 and α3 GlyRs

Compound	α1 GlyR IC_{50} (μM)	α3 GlyR IC_{50} (μM)
6/7	>200	67 ± 16[a]
9	25.9 ± 5.3[*b]	>300
11a/b	8.8 ± 0.5[*c]	33.9 ± 7.0[*d]

[*] $p < 0.01$; [a] $n_H = 0.5 \pm 0.1$; [b] $n_H = 0.8 \pm 0.1$; [c] $n_H = 1.0 \pm 0.1$; [d] $n_H = 0.8 \pm 0.1$. All results averaged from 4–10 cells.

A structure activity relationship analysis inspired by the monomeric alkaloid natural products **5**–**8**, and further informed by the synthetic alkaloid analogs **10**, **11a/b** and **12a/b**, provides a sense of the molecular characteristics needed for GlyR potency and isoform selectivity. For example, conversion of the 3′-imino to a 3′-oxo moiety (**5** to **6/7**, and **12a/b** to **11a/b**) leads to a dramatic increase in potency. Likewise, the level of *N*-methylation plays a critical role in both potency and isoform selectivity with the unmethylated **10** being inactive, the 2′-*N*-methylated **11a/b** being selectively potent against α1 GlyRs, and the 2′,4′-*N*,*N*-dimethylated **6/7** being selectivity potent against α3 GlyRs. Interestingly, reduction of $\Delta^{8,1'}$(**8**) abolished all activity against both α1 and α3 GlyRs.

3. Conclusion

In summary, our investigations confirm that marine biodiscovery offers a valuable approach to discover new classes of GlyR modulators. Following the screening of a library of marine extracts, we identified a southern Australian marine sponge, *Ianthella* cf. *flabelliformis* as a priority extract for the discovery of small molecule GlyR modulators. Bioassay guided fractionation yielded the structurally diverse sesquiterpenes **1**–**4** and indole alkaloids **5**–**9**, with the GlyR modulatory activity detected in *Ianthella* cf. *flabelliformis* being attributed to the alkaloids **6/7** and **9**. That these sponge alkaloids inhibited GlyR with apparently "tunable" selectivity for either α1 or α3 GlyRs, prompted the one-pot synthesis of alkaloids **10**, **11a/b** and **12a/b**, leading to the discovery of the readily accessible and more potent α1 selective GlyR antagonists.

4. Experimental

4.1. General Experimental Details

Optical rotations were measured on a JASCO P-1010 polarimeter. UV-vis spectra were obtained on a Cary 50 UV-visible spectrophotometer. NMR experiments were performed on a Bruker Avance DRX600. Chemical shifts were calibrated internally against residual solvent signals (DMSO-d_6: δ_H = 2.50, δ_C = 39.5; $CDCl_3$: δ_H = 7.26, δ_C = 77.0; CD_3OD: δ_H = 3.30, δ_C = 49.2). ESIMS were recorded using an Agilent 1100 Series separations module equipped with an Agilent 1100 Series LC/MSD mass detector in both positive and negative ion modes. HRESIMS measurements were obtained on a Bruker micrOTOF mass spectrometer by direct infusion in MeCN at 3 μL/min flow using sodium formate clusters as an internal calibrant. HPLC was performed using an Agilent 1100 series HPLC controlled using ChemStation Rev.B.02.01. All chemicals were purchased from Merck, Sigma-Aldrich or Fluka. Solvents used for general purposes were of at least analytical grade, and solvents used for HPLC were of HPLC grade. Agilent Zorbax C_3 and C_8 250 × 9.4 mm columns were used for HPLC analyses and separations.

4.2. Marine Extracts Library

A library of >2500 marine invertebrate and alga samples, collected from intertidal, coastal and deep sea locations across southern Australia and Antarctica, were processed to generate an extract library suitably formatted for medium to high throughput bioassay. A portion (7 mL) of the archived EtOH extract of each marine sample was decanted, concentrated *in vacuo*, weighed and partitioned into *n*-BuOH (2 mL) and H_2O (2 mL). This pre-processing achieves a >10 fold concentration of "drug-like" small molecules, while simultaneously desalting and simplifying the solubility characteristics of, the *n*-BuOH solubles. Aliquots (1 mL) of both *n*-BuOH and H_2O phases were transferred to deep 96-well plates, to generate a set of extract library plates. These plates were subsequently used to prepare 10- and 100-fold dilution plates.

4.3. Sponge Collection and Taxonomy

Sponge specimen CMB-03322 was collected by SCUBA from Lonsdale Wall, The Rip, Port Phillip Heads, Victoria (38° 17′ 55″ S, 144° 37′.46″ E). A description of the specimen is as follows: Growth form massive-thickly flabelliform; colour in EtOH likely to be an aerophobic colour change to dark purple; texture barely compressible, harsh, fibrous; oscules scattered, sunken; surface opaque, glossy, conulose; spicules none; ectosome thick collagen with fibres tangential or protruding the surface; choanosome a reticulation of fibres strongly laminated and pith visible. Large primary fibres cored by single column of sand grains, smaller fibres clear of detritus. The sponge was identified as *Ianthella* cf. *flabelliformis* (Order Verongida, Family Ianthellidae) and a type specimen registered with Museum Victoria (Registry No. MVF166222).

4.4. Extraction and Fractionation

A portion (350 mL) of the aqueous EtOH extract of the *Ianthella* cf. *flabelliformis* was decanted and concentrated *in vacuo* to return a black solid (1.74 g), which was subsequently partitioned between *n*-BuOH (3 × 50 mL) and H_2O (50.0 mL). GlyR bioassays (see below) established that all activity was concentrated in the *n*-BuOH solubles (519.7 mg), which were sequentially triturated with 2 × 15 mL aliquots of hexane, CH_2Cl_2 and MeOH, and concentrated *in vacuo* to return 9.0, 283.0 and 74.6 mg yields respectively. A portion of the CH_2Cl_2 soluble fraction (130 mg) was subjected to HPLC fractionation (Zorbax C_8 5 μm 250 × 9.4 mm column, 4 mL/min, gradient elution of 10–100% MeCN/H_2O over 25 min, with an isocratic 0.01% TFA/H_2O modifier) to yield ianthellalactam A (**1**) (t_R = 12.9 min; 2.6 mg, 0.056%), ianthellalactam B (**2**) (t_R = 13.3 min; 1.7 mg, 0.032%), dictyodendrillin (**3**) (t_R = 13.9 min; 0.2 mg, 0.003%), aplysinopsin (**5**) (t_R = 7.0 min; 2.4 mg, 0.041%), 8*E*-3′-deimino-3′-oxoaplysinopin (**6**) (t_R = 10.1 min; 2.7 mg, 0.051%), 8Z-3′-deimino-3-oxoaplysinopin (**7**) (t_R = 10.6 min; 3.5 mg, 0.067%), dihydroaplysinopsin (**8**) (t_R = 6.4 min; 1.8 mg, 0.034%) and tubastrindole B (**9**) (t_R = 5.8 min; 1.7 mg, 0.029%). Since the MeOH soluble fraction exhibited a similar HPLC-DAD and ^{1}H NMR profile to the CH_2Cl_2 soluble fraction, the remaining CH_2Cl_2 (153.0 mg) and MeOH solubles (74.6 mg) were combined and fractionated using the method outlined above, to yield **1**–**3** and **5**–**9** together with a new minor metabolite/artifact, ethyl dictyodendrillin (**4**) (t_R = 14.2 min; 1.7 mg, 0.029%). Although the geometric isomers 8*E*-3′-deimino-3′-oxoaplysinopsin (**6**) and 8*Z*-3′-deimino-3′-oxoaplysinopsin (**7**) were well resolved by HPLC, the isomers rapidly isomerized during handling (and on exposure to light). Isolation in a darkened laboratory, followed by rapid data acquisition, did permit independent characterization of these photolabile isomers. Note – yields for all isolated compounds were calculated as a weight-to-weight estimate against the crude *n*-BuOH solubles

4.5. Characterization of Natural Products

4.5.1. ianthellalactam A (1)

Pale yellow oil. UV-vis (MeOH) λ_{max} (log ε) 203 nm (4.33); NMR (600 MHz, methanol-d_4) see Table 1 and Supporting Information Figures S1a–b and Table S1; HRESI(+)MS *m/z* 314.1721 (calcd. for $C_{17}H_{25}NO_3Na$ 314.1727).

4.5.2. ianthellalactam B (2)

Pale yellow oil. UV-vis (MeOH) λ_{max} (log ε) 202 nm (4.40); NMR (600 MHz, methanol-d_4) see Table 1 and Supporting Information Figures S2a–b and Table S2; HRESI(+)MS *m/z* 314.1725 (calcd. for $C_{17}H_{25}NO_3Na$ 314.1727).

4.5.3. dictyodendrillin[13] (3)

Colorless oil. ^{1}H NMR (600 MHz, $CDCl_3$) see Supporting Information Figures S3a–b. ESI(+)MS *m/z* 251 $[M+H]^+$, ESI(–) MS *m/z* 249 $[M-H]^-$. Identical with an authentic sample of dictyodendrillin.[13]

4.5.4. ethyl dictyodendrillin (4)

Colorless oil. UV-vis (MeOH) λ_{max} (log ε) 204.9 (4.27), 201 (4.27); NMR (600 MHz, $CDCl_3$) see Supporting Information Figures S4a–b and Table S4.

4.5.5. aplysinopsin[14] (5)

Yellow solid**.** UV-vis (MeOH) λ_{max} (log ε) 217 (4.0), 279 (3.49), 391 (3.67); NMR (600 MHz, DMSO-d_6) see Supporting Information Figures S5a–b and Table S5; HRESI(+)MS *m/z* 255.1247 (calcd. for $C_{14}H_{15}N_4O$ 255.1240). Identical with an authentic sample of aplysinopsin.[14]

4.5.6. 8*E*-3′-deimino-3′-oxoaplysinopsin[15] (6)

Yellow solid. UV-vis (MeOH) λ_{max} (log ε) 203 (4.01), 278 (3.49), 367 (3.83) nm; NMR (600 MHz, DMSO-d_6) see Supporting Information Figures S6a–b and Table S6; HRESIMS *m/z* 278.0909 (calcd. for $C_{14}H_{13}N_3O_2Na$ 278.0900).

4.5.7. 8*Z*-3′-deimino-3′-oxoaplysinopsin[15] (7)

Yellow solid. UV-vis (MeOH) λ_{max} (log ε) 203 (4.01), 218 (4.23), 278 (3.49), 367 (3.83) nm; NMR (600 MHz, DMSO-d_6)

see Supporting Information Figures S6a–b and Table S7; HRESIMS *m/z* 278.0909 (calcd. for $C_{14}H_{13}N_3O_2Na$ 278.0900).

4.5.8. dihydroaplysinopsin[16] (8)

Yellow solid. $[\alpha]_D^{23}$ –86 (*c* 0.05 MeOH); UV-vis (MeOH) λ_{max} (log ε) 202 (3.98), 218 (3.93), 280 (3.12) nm; NMR (600 MHz, DMSO-d_6) see Supporting Information Figures S8a–b and Table S8; HRESI(+)MS *m/z* 257.1393 (calcd. for $C_{14}H_{17}N_4O$ 257.1397).

4.5.9. tubastrindole B[17] (9)

Yellow solid. $[\alpha]_D^{23}$ –44 (*c* 0.1 MeOH); UV-vis (MeOH) λ_{max} (log ε) 202 (4.21), 217 (4.27), 205 (4.24), 268 (3.55) nm; NMR (600 MHz, DMSO-d_6) see Supporting Information Figures S9a–b and Table S9; HRESI(+)MS *m/z* 509.2415 (calcd. for $C_{28}H_{29}N_8O_2$ 509.2408).

4.6. Synthesis of Analogs

4.6.1. General Synthetic Procedures

Solutions of indole-3-carboxaldehyde (1.0 g, 6.9 mmol) and either hydantoin, methyl hydantoin or creatinine (17 mmol, 2.5 equiv.) in piperidine (5 mL) were refluxed for 45 min under argon. The solutions were then cooled to room temperature and diluted with acetone (10 mL). The resulting yellow precipitates were filtered and washed with cold acetone (10 mL) to yield the essentially pure 8*E* isomers (**10**, **11a** and **12a**). Suspensions of **11a** and **12a** in methanol were exposed to UV light for 3 h, yielding ~1:1 mixtures of the 8*E* and 8*Z* (**11b** and **12b**) isomers.

4.6.2. 8*E*-3′-deimino-2′,4′-bisdemethyl-3′-oxoaplysinopsin[18] (10)

Yellow solid (0.90 g, 57%). UV-vis (MeOH) λ_{max} (log ε) 227.1 (4.03), 277.9 (3.55), 364 (4.09) nm; NMR (600 MHz, methanol-d_4) see Supporting Information Figures S10a–b and Table S10; HRESIMS *m/z* 250.0593 (calcd. for $C_{12}H_9N_3O_2Na$ 250.0587).

4.6.3. 8*E*-3′-deimino-4′-demethyl-3′-oxoaplysinopsin[19] (11a).

Yellow solid (0.76 g, 46%). UV-vis (MeOH) λ_{max} (log ε) 228.9 (4.01), 276 (3.49) 336.9 (3.83) nm; NMR (600 MHz, methanol-d_4) see Supporting Information Figure S11a and Table S11a; HRESIMS *m/z* 264.0746 (calcd. for $C_{13}H_{11}N_3O_2Na$ 264.0743).

4.6.4. 8*Z*-3′-deimino-4′-demethyl-3′-oxoaplysinopsin[19] (11b).

Yellow solid. UV-vis (MeOH) λ_{max} (log ε) 228.9 (4.01), 276 (3.49) 336.9 (3.83) nm; NMR (600 MHz, methanol-d_4) see Supporting Information Figure S11b and Table S11b; HRESIMS *m/z* 264.0746 (calcd. for $C_{13}H_{11}N_3O_2Na$ 264.0743).

4.6.5. 8*E*-4′-demethylaplysinopsin[20] (12a).

Yellow solid. (0.70 g, 42%). UV-vis (MeOH) λ_{max} (log ε) 228.9 (3.93), 277.9 (3.49), 387 (3.90) nm; NMR (600 MHz, DMSO-d_6) see Supporting Information Figure 12a and Table S12a; HRESIMS *m/z* 241.1085 (calcd. for $C_{13}H_{13}N_3O$ 241.1084).

4.6.6. 8*Z*-4′-demethylaplysinopsin[20] (12b).

Yellow solid. UV-vis (MeOH) λ_{max} (log ε) 228.9 (3.93), 277.9 (3.49), 387 (3.90) nm; NMR (600 MHz, DMSO-d_6) see Supporting Information Figure 12b and Table S12b; HRESIMS *m/z* 241.1085 (calcd. for $C_{13}H_{13}N_4O$ 241.1084).

4.7. Bioassays

4.7.1. Primary GlyR Screening of Marine Extracts

The initial screen of >2500 marine extracts against recombinantly expressed α1 and α3 GlyRs was performed using a yellow fluorescent protein-based anion flux assay as previously described.[12,21] In this bioassay, 90 µL of each 100-fold diluted *n*-BuOH partition was transferred into one well of a 384-well plate, and was dried under nitrogen. The plates containing dried *n*-BuOH partitions were protected from light and stored at –30 °C until required. On the day of the experiment an aliquot (30 µL) of extracellular solution [NaCl (140 mM), KCl (5 mM), $CaCl_2$ (2 mM), $MgCl_2$ (1 mM), HEPES (10 mM), and glucose (10 mM) (pH 7.4 using NaOH)] was added to each well and mixed/dissolved using a multi-channel pipette. Subsequently, an aliquot (10 µL) of this solution was transferred into the corresponding well of a 384-well plate containing approx. 5000 cells and 15 µL of extracellular solution per well, and incubated at room temperature for 30 min. The 384-well plates were then placed onto the motorized stage of an in-house imaging system[21] and cells were imaged twice: once in 25 µL of extracellular solution containing the *n*-BuOH partition and once 10 s after the injection of 50 µL NaI solution supplemented with 500 µM glycine. The NaI solution was similar in composition to NaCl control solution except the NaCl was replaced by equimolar NaI. Images of fluorescent cells were segmented and quantitatively analyzed using a modified version of DetecTIFF software.[22] In brief, images were segmented using an iterative size and intensity-based thresholding algorithm and the fluorescence signal of identified cells was calculated as the mean of all pixel values within the area of a cell. GlyR activation response was used as a measure of extract potency and was defined as $(F_{init}-F_{final})\times100/F_{init}$, where F_{init} and F_{final} were the initial and final values of fluorescence, respectively. All experiments were performed twice in neighboring wells. Hits were selected by visual inspection of color maps generated by analysis software. For hit confirmation, 24 µL of the corresponding 10-fold diluted *n*-BuOH partition was transferred into a well of a 384-well plate, and was dried and stored as described above. On the day of the experiment the dried 10-fold diluted *n*-BuOH partitions were resuspended in 80 µL extracellular solution as described above and two aliquots each of 17 and 10 µL respectively were then transferred in neighboring wells containing ~5000 cells and 15 µL extracellular solution per well. Imaging and image analysis were conducted as described above. The concentration dependence of the drug effects was used as measure for extract potency and level of prioritization. From these experiments we identified *Ianthella* cf. *flabelliformis* (CMB-03322) as an extract with antagonist activity on α1 and α3 GlyRs.

4.7.2. Automated Electrophysiology

Electrophysiological screening was performed using an automated planar patch-clamp device (Patchliner, Nanion Technologies GmbH, Munich, Germany). Stable α1 and α3 GlyR expressing HEK293 cell lines, produced as previously described,[12,22] were maintained in Minimal Essential medium. After 2–3 days in culture, cells were trypsinized and suspended in extracellular solution [NaCl (140 mM), KCl (4 mM), $CaCl_2$ (2 mM), $MgCl_2$ (1 mM), HEPES/NaOH (10 mM) and glucose (5 mM) (pH 7.4 adjusted with NaOH)] at a density of 1×10^6 cells/mL before injecting into the Patchliner chip. This standard extracellular solution was employed in all Patchliner experiments. The internal solution contained KCl (50 mM), NaCl (10 mM), KF (60 mM), $MgCl_2$ (2 mM), EGTA (20 mM), HEPES/KOH (10 mM) (pH 7.2). All experiments were performed at room temperature. 1 M glycine (Ajax Finechem, Seven Hills, NSW, Australia) stocks were prepared in water and stored at –20 °C. All test compounds (marine natural products and synthetics) were dissolved in DMSO (Sigma-Aldrich) and stored at –20 °C. From these stocks, solutions for experiments were prepared on the day of recording.

4.7.3. Data Analysis

Results are expressed as mean ± standard error of the mean of three or more independent experiments. The Hill equation was used to calculate the half inhibitory concentration (IC_{50}) and Hill coefficient (n_H) values of individual concentration–response relationships. All curves were fitted using a nonlinear least squares algorithm (Sigmaplot 11.0; Jandel Scientific, San Rafael, CA, USA). Statistical significance was determined by unpaired Student's t-test, with $p < 0.05$ representing significance.

Acknowledgments

We thank L. Goudie for taxonomic identification of marine sponges and acknowledge the generous support of an Australian Development Scholarship (W.B) and a University of Queensland Scholarship (R.I). This research was funded in part by the Institute for Molecular Bioscience, the Queensland Brain Institute, The University of Queensland, the National Health and Medical Research Council (project grant #613448) and the Australian Research Council (LP120100088).

References and notes

1. Lynch, J. W. *Physiol. Rev.* **2004**, *84*, 1051.
2. Harvey, R. J.; Depner, U. B.; Wassle, H.; Ahmadi, S.; Heindl, C.; Reinold, H.; Smart, T. G.; Harvey, K.; Schutz, B.; Abo-Salem, O. M.; Zimmer, A.; Poisbeau, P.; Welzl, H.; Wolfer, D. P.; Betz, H.; Zeilhofer, H. U.; Muller, U. *Science* **2004**, *304*, 884.
3. Haverkamp, S.; Muller, U.; Harvey, K.; Harvey, R. J.; Betz, H.; Wassle, H. *J. Comp. Neurol.* **2003**, *465*, 524.
4. Haverkamp, S.; Muller, U.; Zeilhofer, H. U.; Harvey, R. J.; Wassle, H. *J. Comp. Neurol.* **2004**, *477*, 399.
5. Heinze, L.; Harvey, R. J.; Haverkamp, S.; Wassle, H. *J. Comp. Neurol.* **2007**, *500*, 693.
6. Weltzien, F.; Puller, C.; O'Sullivan, G. A.; Paarmann, I.; Betz, H. *J. Comp. Neurol.* **2012**, *520*, 3962.
7. Webb, T. I.; Lynch, J. W. *Curr. Pharm. Des.* **2007**, *13*, 2350.
8. Xiong, W.; Cui, T.; Cheng, K.; Yang, F.; Chen, S. R.; Willenbring, D.; Guan, Y.; Pan, H. L.; Ren, K.; Xu, Y.; Zhang, L. *J. Exp. Med.* **2012**, *209*, 1121.
9. Manzke, T.; Niebert, M.; Koch, U. R.; Caley, A.; Vogelgesang, S.; Hulsmann, S.; Ponimaskin, E.; Muller, U.; Smart, T. G.; Harvey, R. J.; Richter, D. W. *J. Clin. Invest.* **2010**, *120*, 4118.
10. Eichler, S. A.; Kirischuk, S.; Juttner, R.; Schaefermeier, P. K.; Legendre, P.; Lehmann, T. N.; Gloveli, T.; Grantyn, R.; Meier, J. C. *J. Cell Mol. Med.* **2008**, *12*, 2848.
11. Chung, S. K.; Vanbellinghen, J. F.; Mullins, J. G.; Robinson, A.; Hantke, J.; Hammond, C. L.; Gilbert, D. F.; Freilinger, M.; Ryan, M.; Kruer, M. C.; Masri, A.; Gurses, C.; Ferrie, C.; Harvey, K.; Shiang, R.; Christodoulou, J.; Andermann, F.; Andermann, E.; Thomas, R. H.; Harvey, R. J.; Lynch, J. W.; Rees, M. I. *J. Neurosci.* **2010**, *30*, 9612.
12. Balansa, W.; Islam, R.; Fontaine, F.; Piggott, A. M.; Zhang, H.; Webb, T. I.; Gilbert, D. F.; Lynch, J. W.; Capon, R. J. *Bioorg. Med. Chem.* **2010**, *18*, 2912.
13. Tran, N. H.; Hooper, J. N. A.; Capon, R. J. *Aust. J. Chem.* **1995**, *48*, 1757.
14. Kazlauskas, R.; Murphy, P. T.; Quinn, R. J.; Wells, R. J. *Tetrahedron Lett.* **1977**, *18*, 61.
15. Guella, G.; Mancini, I.; Zibrowius, H.; Pietra, F. *Helv. Chim. Acta* **1988**, *71*, 773.
16. Okuda, R. K.; Klein, D.; Kinnel, R. B.; Li, M.; Scheuer, P. J. *Pure Appl. Chem.* **1982**, *54*, 1907.
17. Iwagawa, T.; Miyazaki, M.; Okamura, H.; Nakatani, M.; Doe, M.; Takemura, K. *Tetrahedron Lett.* **2003**, *44*, 2533.
18. Rashid, M. A.; Gustafson, K. R.; Cardellina, J. H., II; Boyd, M. R. *J. Nat. Prod.* **1995**, *58*, 1120.
19. Jakse, R.; Recnik, S.; Svete, J.; Golobic, A.; Golic, L.; Stanovnik, B. *Tetrahedron* **2001**, *57*, 8395.
20. Djura, P.; Faulkner, D. J. *J. Org. Chem.* **1980**, *45*, 735.
21. Kruger, W.; Gilbert, D.; Hawthorne, R.; Hryciw, D. H.; Frings, S.; Poronnik, P.; Lynch, J. W. *Neurosci. Lett.* **2005**, *380*, 340.
22. Gilbert, D.; Esmaeili, A.; Lynch, J. W. *J. Biomol. Screen.* **2009**, *14*, 86.

Supplementary Material

Chemical profiling, isolation schemes and spectroscopic data for compounds **1**–**13** can be found, in the online version, at doi:XX.XXXX/j.bmc.2013.XX.XXX.

Figure 1

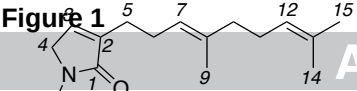

ianthellalactam A (**1**)

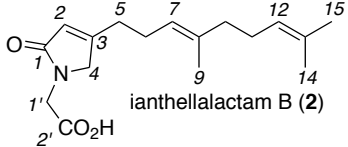

ianthellalactam B (**2**)

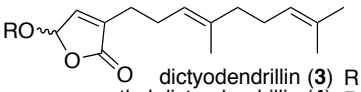

dictyodendrillin (**3**) R = H
ethyl dictyodendrillin (**4**) R = Et

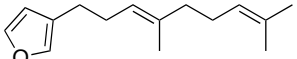

dendrolasin (**13**)

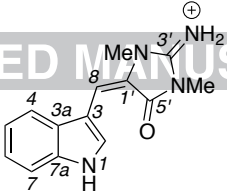

aplysinopsin (**5**)
TFA salt

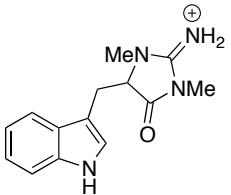

dihydroaplysinopsin (**8**)
TFA salt

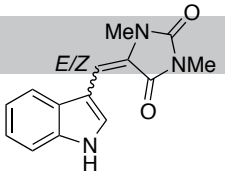

8*E*-3'-deimino-3'-oxoaplysinopsin (**6**)
8*Z*-3'-deimino-3'-oxoaplysinopsin (**7**)

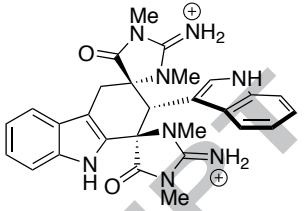

tubastrindole B (**9**)
TFA salt

Figure 2

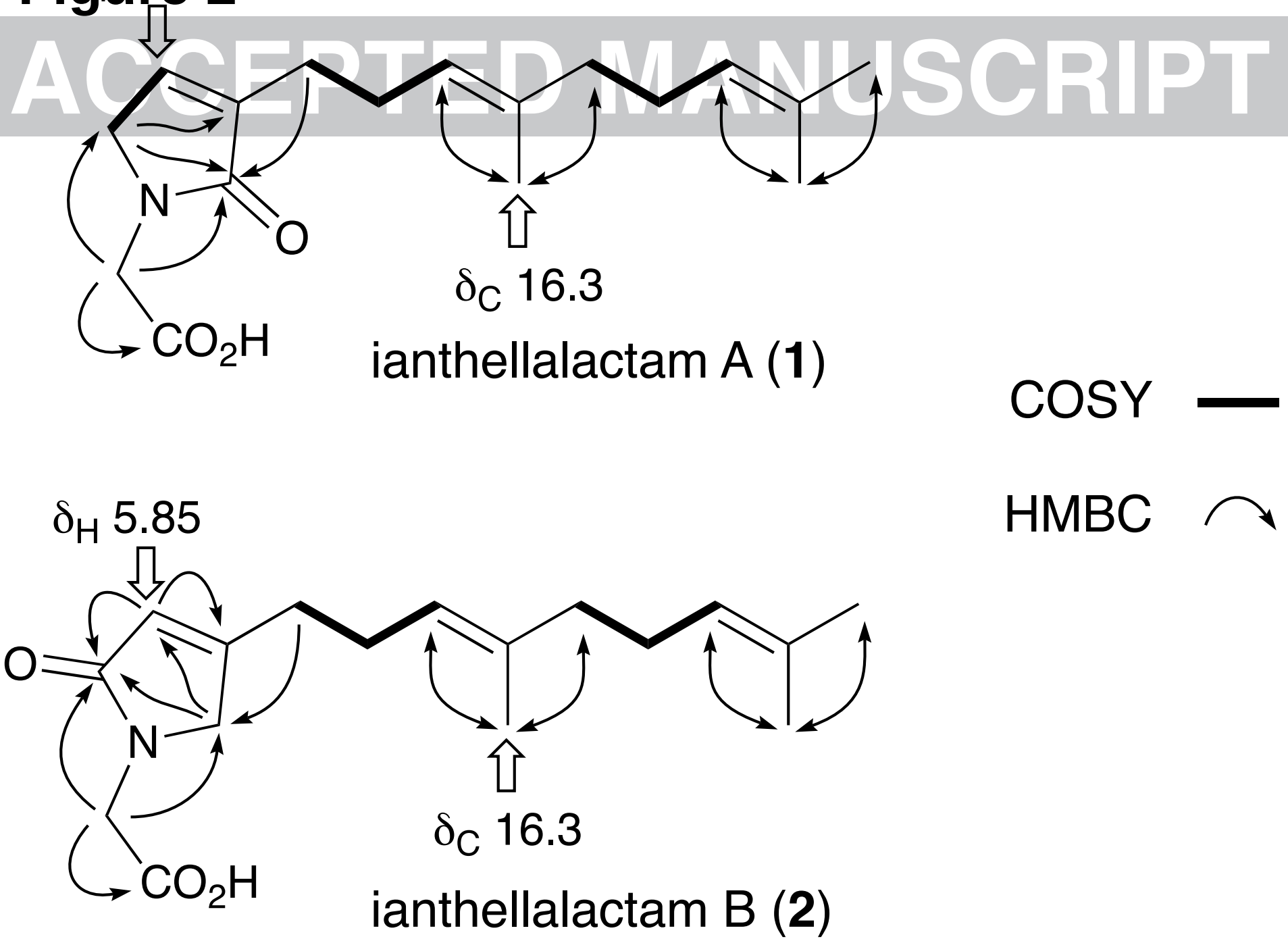

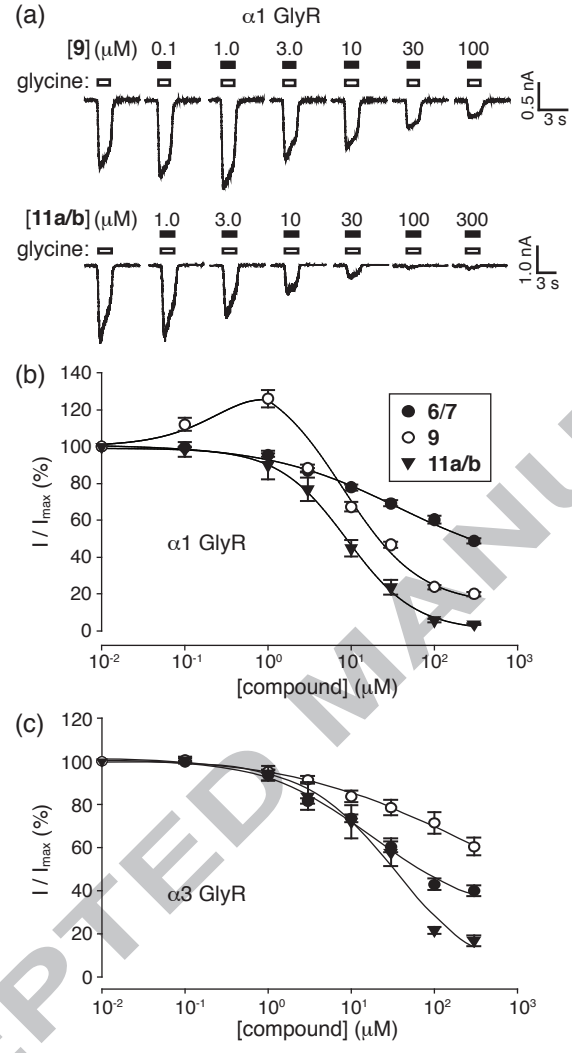
(a)
α1 GlyR
[9] (μM) 0.1 1.0 3.0 10 30 100
glycine:
0.5 nA
3 s
[11a/b] (μM) 1.0 3.0 10 30 100 300
glycine:
1.0 nA
3 s
(b)
6/7
9
11a/b
α1 GlyR
I / Imax (%)
[compound] (μM)
(c)
α3 GlyR
I / Imax (%)
[compound] (μM)

Figure 4